J. Plasma Physics (2013), *vol.* 79, *part* 3, *pp.* 295–303. © Cambridge University Press 2012
doi:10.1017/S002237781200092X

Prediction of potential well structure formed in spherical inertial electrostatic confinement fusion devices with various parameters

M. GHASEMI, M. HABIBI and R. AMROLLAHI

Faculty of Nuclear Engineering and Physics, Amirkabir University of Technology, 424 Hafez Ave, Tehran, Iran
(mghasemi@aut.ac.ir)

(Received 13 July 2012; revised 18 September 2012; accepted 20 September 2012; first published online 26 November 2012)

Abstract. In this paper, the theoretical analysis regarding potential structure on the inertial electrostatic confinement fusion devices has been carried out. Negatively biased grid as cathode placed at the center of the device surrounded by anode is assumed. The device is an ion-injection system and electrons may be emitted from the surface of the cathode. So the existence of both ion and electron currents inside the cathode is considered. Dependence of radial potential well structure on some important parameters as the spreads in the normalized total and angular electron and ion energies, the ratio of ion circulating current to electron circulating current, ion perveance, and grid transparency are investigated by solving Poisson equation.

1. Introduction

Inertial electrostatic confinement (IEC) assumes that charged particles are electrostatically confined within a potential well. In IEC fusion (IECF) devices, charged particles (ions and electrons) are injected radially inward to the center, trapping species in the electrostatic field, and reaching the dense core where fusion reactions are expected to take place. This strong ion-concentration at the center of the potential well is the defining feature of IEC. Therefore, formation of a spherical potential well is needed to provide electrostatic confinement.

These devices have many potential applications. They have been used as a commercial neutron generator for industrial applications. The other applications include medical isotope production, inspection, oil well logging, detection of explosives, breeding advanced fuels, and some other usages. There is some uncertainty that it can be used as fusion power generating but it can replace neutron sources in certain diagnostics and analytical applications (Kulcinski 1996; Cipiti and Kulcinski 2003; Weidner 2003).

The advantages of IECF devices are that they are small, low cost, easy to construct, high performance, suitable for exploring in this field, and also their shielding requirements are limited. They can be dangerous because of high voltage and harmful radiation sources.

Creation of electrostatic potential wells is necessary for ions confinement and fusion reactions. Also IEC arrangements require the creation of spherical potential well and depend on well structure. Theoretical studies and predictions in this field have significant effect on confining energetic ions for fusion purposes to improve these devices.

The aim of this paper is to predict potential well structure formed in IECF devices with various conditions by solving Poisson equation. The analysis of the potential profile and numerical results is described. Finally, a discussion and conclusions are presented.

2. Review of previous researches

Numerous experimental and theoretical studies have been performed regarding the potential well structure within IECF devices. Using electrostatic confinement for producing fusion neutrons was suggested by Farnsworth (1966).

Elmore et al. (1959) discussed about proposing IEC application at thermonuclear reactor. They assumed a spherical IEC system in which electrons were radially directed toward the center. The theoretical studies of the equilibrium and stability of plasma have been carried out in this system.

Hirsch (1967, 1968) studied fusion reaction in IECF device and suggested the potential multi-well structure in spherical IECF device. A mono-energetic ion and electron distribution functions were assumed in theoretical studies. His experiments with an ion-injected spherical IECF device showed high neutron generation. Neutron and X-ray data collected by Hirsch specified the existence of double potential well structure within his device.

Hockney (1968) showed that stable double potential well structures can be formed inside a cylindrical IEC device by the injection of a single species of charged particles.

Dolan et al. (1972) studied potential well structure as a function of radius for spherical and cylindrical geometries theoretically ignoring collision effect. Two-species injection including spreads in energy and angular momentum was assumed. They did not predict irregular potential wells. Experimental work was carried out using neon and deuteron gases. The theoretical predictions based on electron density distributions are confirmed by their experimental results.

Swanson et al. (1973a) used electron-beam probing to study the behavior of potential wells formed by electron injection in an IECF device indicating that a double potential structure may exist in agreement with Hirsch's (1968) claim.

Swanson et al. (1973b) carried out experiments to study the potential structure produced within a highly open spherical anode when electrons are injected under conditions of high vacuum and low-pressure deuterium background gas. Their results showed the formation of a multiple potential well structure.

Black and Klevans (1974) performed theoretical studies to describe the behavior of an ion-injected IECF device. Electrons and ions were divided into three energy groups. Their analysis showed only a single well formation.

Black and Robinson (1974) developed an electron-beam probe to measure the potential profile of plasma within a spherical grid structure, which was designed to trap charged particles. For a variety of experimentally controlled plasma parameters, no measurable departures from electrostatic potential profiles were observed.

Hu and Klevans (1974) presented the theoretical model of ion-injection IECF device and tried to find the conditions necessary to prepare the multiple potential well theories.

Swanson (1975) and Dolan (1975) developed the theoretical models for electron-injected IECF devices, considering energy spreads and angular momentum for particles. Swanson's calculations showed double potential well structure.

Cherrington and Swanson (1977) performed the theoretical studies on the potential structure including spreads in the total energy and the angular energies of the injected ion and electron. They obtained the multiple potential well structures.

Nadler (1992) measured proton source rate profile with collimated proton detector and claimed the existence of a single potential well.

Wong and Krall (1992) studied theoretically the potential well structure produced by injection of electrons.

Nevins (1995) studied the IECF systems on a non-equilibrium ion distribution function. The collisional relaxation time required to maintain an IEC reactor for beyond the ion-ion collisional timescale was greater than the produced fusion power. He discussed the possibility of IEC for the development of commercial electric power plants.

Tzonev et al. (1996) showed that high-current ion beams having large-angular-momentum spread can also form deep potential well traps.

Thorson et al. (1997) measured the electrostatic potential distribution using emissive probes. Their measurements showed a virtual anode in the converged core region. No virtual cathode and multiple potential well structure in the core were found.

Ohnishi et al. (1997) studied the correlation between potential well structure and neutron production in IECF.

Yamamoto et al. (1997) discussed characteristics of double-grid discharges and compared with single-grid experiments.

Ohnishi et al. (1998) discussed the experiments and numerical simulations for scaling of neutron injection versus ion currents. The numerical simulation gave stronger scaling versus ion current. They claimed to verify the numerically estimated simulation the experiments in higher ion current regime required.

Gu and Miley (2000) detected a double potential well using a high-resolution proton collimator.

Matsuura et al. (2000) calculated the potential well structure by solving the Poisson equation for fixed ion and electron distribution functions. They evaluated the neutron production rate and showed that a double potential well structure is not necessary to produce double radial peaks in the neutron production rate.

Matsuura et al. (2001) investigated the radial profile of neutron production rate considering both the beam-beam and beam-target fusions. The potential well structure was obtained and neutron production rate was evaluated. They showed that the total neutrons produced by beam-beam fusion are lower than beam-target fusion.

Momota and Miley (2001) computed the radial potential distribution for a collisionless, ion-injected system. They were able to generate double potential well structures and found that the relative depth of a double well increased as the relative focusing of electrons to ions improved.

Matsuura et al. (2003) studied the correlation between the ion-distribution function and the neutron production in IECF by introducing an equation for ion and electron distribution functions and solving Poisson equation. Dependence of the total neutron production rate on current discharge for several combinations of the ion and electron was discussed. They showed that if electrons have high convergence and energetic component in comparison with ions, the neutron production can increase in proportion to more than a power of discharge current. So it was predicted that potential structure is strongly dependent on the device parameter such as current, voltage, and ion and electron convergence.

Matsuo et al. (2004) evaluated the correlation between the proton-distribution function and the discharge current in D-3He IECF device by using Poisson equation. They showed that if electrons have high convergence and energetic component in comparison with ions, the proton production can increase in proportion to more than a power of discharge current even more easily for higher discharged voltage than that for deuterium gas system. So it was predicted that potential structure is strongly dependent on the device parameter such as current voltage and ion and electron convergence.

Meyer et al. (2005) reviewed the previous work of potential structure in IECF devices. They classified the systems according to arrangement of electrodes and injected particles and calculated the Poisson equation to evaluate potential well structure for them.

Nebel et al. (2005) performed theoretical and experimental studies of kinetic equilibrium and stability of the virtual cathode in an electron-injected IEC device.

Yoshinaga et al. (2006) studied the energy-distribution function of fast neutron in IECF by solving the Boltzmann equation. The calculated broadness of the ion-distribution function was compared with previous experiments.

Evstatiev et al. (2007) developed the formalism that allows neutralization to occur and describes proper way to inject electrons from the boundary of IECF device to achieve desired electron-density profile.

Taniuchi et al. (2010) studied the effects of grid cathode structure on neutron production rate in low-input-power IECF device experimentally and theoretically. Their experiments showed that the neutron production rate increased by increasing the number of rings (decreasing transparency). They showed that the increase in kinetic energy for the ions by increasing the number of rings, rather than the increase in recirculation ion current, is effective in increasing neutron production rate.

3. Physical properties and computational method

In this paper, we simulate the region inside the cathode for ion-injection system. This system consists of two spherical grids inside a vacuum chamber. Negatively biased grid as cathode is placed at the center and surrounded by the anode. The accelerating fields and potential well provided by grids or virtual cathodes cause the charged ions to accelerate radially inward to the center of the inner grid. During this process, the ions trapped in the electrostatic field collide and fuse with ions coming from the other direction and produce fusion reaction in the dense core. Electrons may be emitted from the surface of the cathode. Also if ionization happens within the cathode, electrons can be produced in this region. So ions and electrons can coexist within the cathode.

Not only the creation of electrostatic potential wells is necessary for ions confinement and fusion reactions but also the IEC arrangements require the creation of spherical potential well and depend on well structure.

Analyzed IECF device in this work with the single potential well structure and ion-density profile is shown in Fig. 1.

Charged ions are accelerated radially inward to the center of the inner grid and are decelerated outward again. The circulating ions will form a virtual anode.

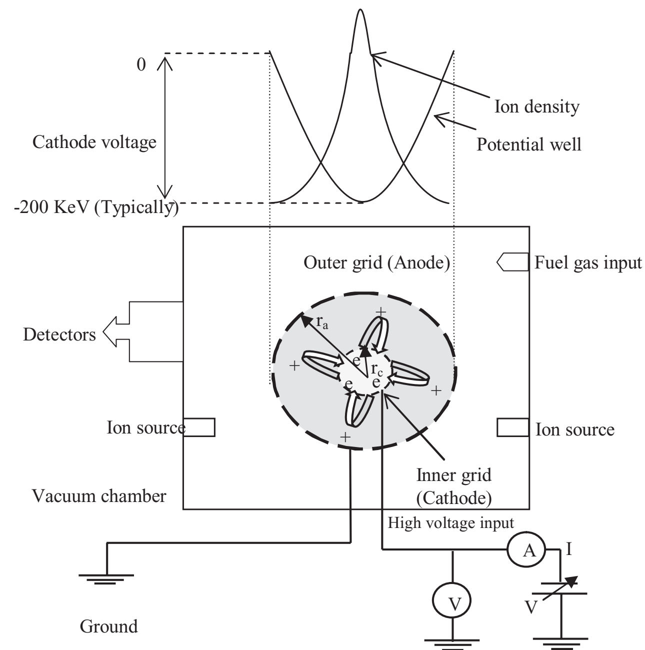

Figure 1. Analyzed IECF device in this work.

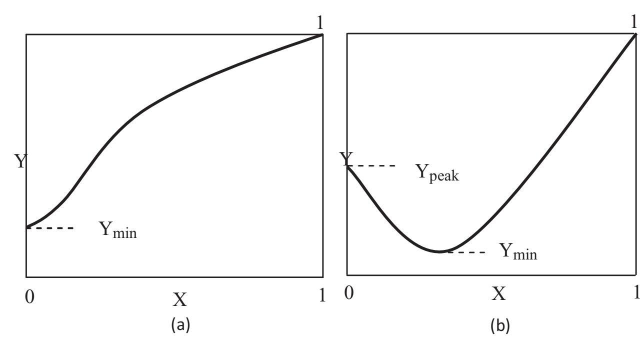

Figure 2. Single (a) and double (b) potential well structures. (Y is the normalized potential at normalized radius, X).

The electrons emitted from the cathode also will be accelerated toward the virtual anode and converge at the center until the electrostatic forces cause the electrons to drive back each other, and are thought to create a virtual cathode inside the area of the virtual anode. Some ions from the virtual anode will be accelerated through the virtual cathode and form the second virtual anode. An infinite number of alternating virtual electrodes will form in this way. It is predicted that the multiple potential wells will appear, and fusion reaction is efficiently induced by accelerated ions trapped in the multiple well structure. Therefore fusion in the wells will increase. In Fig. 2, single and double potential well structures are illustrated. In this figure, Y is the normalized potential at normalized radius, X.

One dimension potential well structure as a function of radius has been found for spherical IEC device where the inner grid voltage is negative.

The distribution functions depend on many factors, including ionization, charge exchange, particle deviations at the grids, particle loss to the grid, particle emission from the grid, recombination of ions and electrons, and loss of particles that are too energetic to be trapped.

If the collision frequency and the fusion reaction rate in comparison with transient frequency of charged particles in the electrostatic potential field are low, the IECF device is a weak collisional system and can be assumed collisionless. For collisionless system, the potential structure may be obtained by solving Poisson equation and the motion of charged particles in an electrostatic potential field, which is described by total energy and angular momentum. For this purpose the Poisson equation is given by

$$\nabla^2 V(r) = \frac{1}{r^2}\frac{d}{dr}\left(r^2\frac{dV(r)}{dr}\right) = \frac{1}{\varepsilon_0}(\rho_e - \rho_i) \tag{3.1}$$

Where ρ_e and ρ_i are electron- and ion-charged distributions, respectively, and ε_0 is the permittivity of free space. This equation is solved with the equations of motion for the ions and electrons.

The total energies of electrons and ions are obtained by conservation of energy and are as follows:

$$-eW_e = \frac{1}{2}\mathrm{m_e}v_{er}^2 + \frac{1}{2}\mathrm{m_e}v_{eQ}^2 - eV(r) \tag{3.2}$$

$$eW_i = \frac{1}{2}\mathrm{m_i}v_{ir}^2 + \frac{1}{2}\mathrm{m_i}v_{iQ}^2 + eV(r) \tag{3.3}$$

In these equations, $-\mathrm{e}W_e$ and $\mathrm{e}W_i$ are the total energies of electrons and ions, v_{er} and v_{ir} are the electron and ion radial velocities, and v_{eQ} and v_{iQ} are the angular velocities of the electron and ion, respectively.

The cathode voltage is defined as $-V_c$. So, for ion born with zero kinetic energy on the inner surface of the cathode, the total energy of the ion ($\mathrm{e}W_i$) will be $-\mathrm{e}V_c$. Within the cathode, the minimum total energy of the ion is $\mathrm{e}V$. Also total energy of ion born at the anode is zero. Therefore, the limits of this system at a radius r inside the cathode are $\mathrm{e}V \leqslant \mathrm{e}W_i \leqslant 0$. For electrons born with zero kinetic energy at the radius r, the total energy of the electron ($-\mathrm{e}W_e$) will be $-\mathrm{e}V$. The total energy of the electron with minimum kinetic energy is $\mathrm{e}V_c$. Therefore, the limits of this system on electron are $-\mathrm{e}V \leqslant \mathrm{e}W_e \leqslant \mathrm{e}V_c$.

Also the angular momentums of electrons and ions are given by

$$L_e = \mathrm{m_e}v_{eQ}r \tag{3.4}$$

$$L_{ie} = \mathrm{m_i}v_{iQ}r \tag{3.5}$$

So the angular energies of electrons and ions are as follows:

$$\mathrm{e}S_e = \frac{L_e^2}{2\mathrm{m_e r_a^2}} = \frac{1}{2}\mathrm{m_e}v_{eQ}^2\left(\frac{r^2}{\mathrm{r_a^2}}\right) \tag{3.6}$$

$$\mathrm{e}S_i = \frac{L_i^2}{2\mathrm{m_i r_a^2}} = \frac{1}{2}\mathrm{m_i}v_{iQ}^2\left(\frac{r^2}{\mathrm{r_a^2}}\right) \tag{3.7}$$

Where, r_a is the anode radius. The electron and ion currents are as follows:

$$I_e = 4\pi r^2\rho_e(r, S_e, W_e)\, v_{er}(S_e, W_e) \tag{3.8}$$

$$I_i = 4\pi r^2\rho_i(r, S_i, W_i)\, v_{ir}(S_i, W_i) \tag{3.9}$$

Where $\rho_e(r, S_e, W_e)$ and $\rho_i(r, S_i, W_i)$ are charge densities for electron and ion, respectively, and are as follows:

$$\rho_e(S_e, W_e) = \frac{I_e(S_e, W_e)}{4\pi r^2}\left(\frac{\mathrm{m_e}}{2\mathrm{e}}\right)^{\frac{1}{2}}\frac{1}{\left(V - W_e - S_e\frac{\mathrm{r_a^2}}{r^2}\right)^{\frac{1}{2}}} \tag{3.10}$$

$$\rho_i(S_i, W_i) = \frac{I_i(S_i, W_i)}{4\pi r^2}\left(\frac{\mathrm{m_i}}{2\mathrm{e}}\right)^{\frac{1}{2}}\frac{1}{\left(W_i - V - S_i\frac{\mathrm{r_a^2}}{r^2}\right)^{\frac{1}{2}}} \tag{3.11}$$

Also v_{er} and v_{ir} are radial velocities. Their relationships with total energy are as follows:

$$v_{er} = \left(\frac{2\mathrm{e}}{\mathrm{m_e}}\right)^{\frac{1}{2}}\left(V - W_e - S_e\frac{\mathrm{r_a^2}}{r^2}\right)^{\frac{1}{2}} \tag{3.12}$$

$$v_{ir} = \left(\frac{2\mathrm{e}}{\mathrm{m_i}}\right)^{\frac{1}{2}}\left(W_i - V - S_i\frac{\mathrm{r_a^2}}{r^2}\right)^{\frac{1}{2}} \tag{3.13}$$

According to (12) and (13), we achieve $S_{e,\max}$ and $S_{i,\max}$

$$S_{e,max} = \left(\frac{r^2}{\mathrm{r_a^2}}\right)(V - W_e) \tag{3.14}$$

$$S_{i,max} = \left(\frac{r^2}{\mathrm{r_a^2}}\right)(W_i - V) \tag{3.15}$$

So we obtain

$$\rho_e = \int_{-V_c}^{V}\mathrm{d}W_e\int_0^{\left(\frac{r^2}{\mathrm{r_a^2}}\right)(V-W_e)}\mathrm{d}S_e\frac{I_e(S_e, W_e)}{4\pi r^2}\left(\frac{\mathrm{m_e}}{2\mathrm{e}}\right)^{\frac{1}{2}} \times\frac{1}{\left(V - W_e - S_e\frac{\mathrm{r_a^2}}{r^2}\right)^{\frac{1}{2}}} \tag{3.16}$$

$$\rho_i = \int_{-V_c}^{V_a}\mathrm{d}W_i\int_0^{\left(\frac{r^2}{\mathrm{r_a^2}}\right)(W_i-V)}\mathrm{d}S_i\frac{I_i(S_i, W_i)}{4\pi r^2}\left(\frac{\mathrm{m_i}}{2\mathrm{e}}\right)^{\frac{1}{2}} \times\frac{1}{\left(W_i - V - S_i\frac{\mathrm{r_a^2}}{r^2}\right)^{\frac{1}{2}}} \tag{3.17}$$

Implemented normalizations are

$$X = \frac{r}{r_c}, Y = -\frac{V}{V_c}, Y_{eE} = \frac{W_e}{V_c}, Y_{iE} = \frac{S_i}{V_c}, Y_{eQ} = \frac{W_e}{V_c}, Y_{iQ} = \frac{W_i}{V_c} \tag{3.18}$$

The Gaussian distributions are assumed for electron and ion current

$$I_e(Y_{eE}, Y_{eQ}) = \mathrm{C_e}\exp\left(\frac{Y_{eE}-1}{\sigma_{eE}}\right)\exp\left(-\frac{Y_{eQ}}{\sigma_{eQ}}\right) \tag{3.19}$$

$$I_i(Y_{iE}, Y_{iQ}) = \mathrm{C_e}\exp\left(-\frac{Y_{iE}}{\sigma_{iE}}\right)\exp\left(-\frac{Y_{iQ}}{\sigma_{iQ}}\right) \tag{3.20}$$

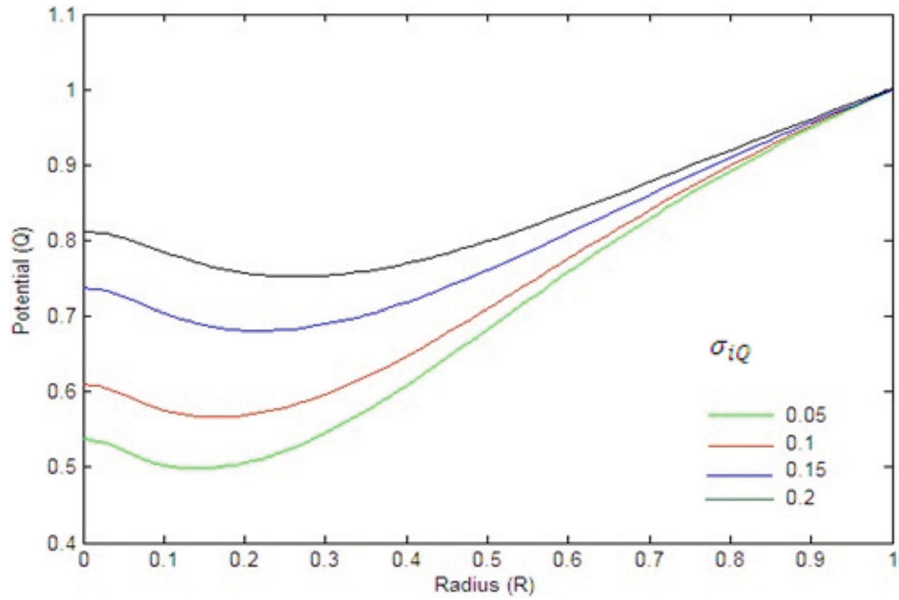

Figure 3. (Colour online) Dependence of radial potential well structure to σ_{i0}. ($\sigma_{eE} = 0.1$, $\sigma_{eQ} = 0.001$, $\sigma_{iE} = 0.05$,$\beta = 0.2$, $P_i = 2$, and $\eta = 0.9$).

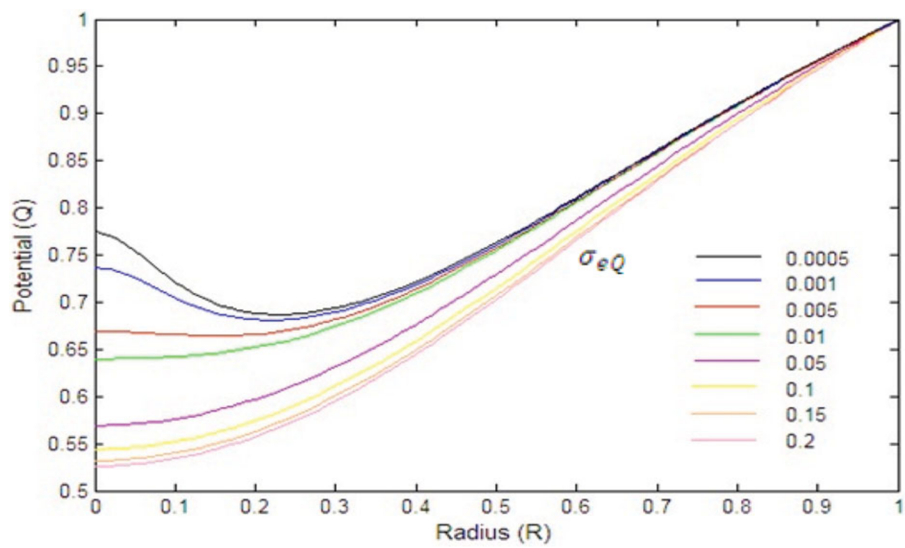

Figure 4. (Colour online) Dependence of radial potential well structure to σ_{e0}. ($\sigma_{eE} = 0.1$, $\sigma_{iE} = 0.05$, $\sigma_{iQ} = 0.15$,$\beta = 0.2$, $P_i = 2$, and $\eta = 0.9$).

Where σ_{eE} and σ_{eQ} are spreads in the normalized total and angular electron energies and σ_{iE} and σ_{iQ} are the spreads in the normalized total and angular ion energies, respectively.

By combining these equations, the final expression of Poisson equation is obtained and is solved numerically using the shooting method with a fourth-order Runge Kutta approximation.

Spreads in the normalized total and angular electron and ion energies ($\sigma_{eE}, \sigma_{eQ}, \sigma_{iE}, \sigma_{iQ}$), the ratio of ion circulating current to electron circulating current (β), ion perveance (($P_i = \frac{I}{V^{3/2}}$), where I is the ion current and V is the cathode voltage) and grid transparency, η, are control variables.

The grid spacing and geometric transparency (η) were varied by changing the number of rings. Grid transparency (η) is defined as the ratio of the open area to the surface area of the spherical grid cathode ($\eta =$ (open area)$/4\pi r_0^2$, where r_0 is the radius of the spherical grid cathode). The perveance P_i connects theoretical and experimental results.

The range $0.1 \leqslant \sigma_{eE} \leqslant 0.5$ for spread in electron total energy has been chosen. Broad distribution for spread in electron angular momentum was chosen in the range $0.0005 \leqslant \sigma_{eQ} \leqslant 0.2$. The chosen broad spread in ion total energies is $0.01 \leqslant \sigma_{iE} \leqslant 0.3$. The ion angular momentum was chosen to be in the range $0.05 \leqslant \sigma_{iQ} \leqslant 0.2$. The range $0.1 \leqslant \beta \leqslant 2$ for β and $0.5 \leqslant P_i \leqslant 3.5$ for P_i are considered. Also the grid transparency is in the range $0.7 \leqslant \eta \leqslant 0.9$.

Variation in radial potential well structure while one control variable is varied and others are constant is

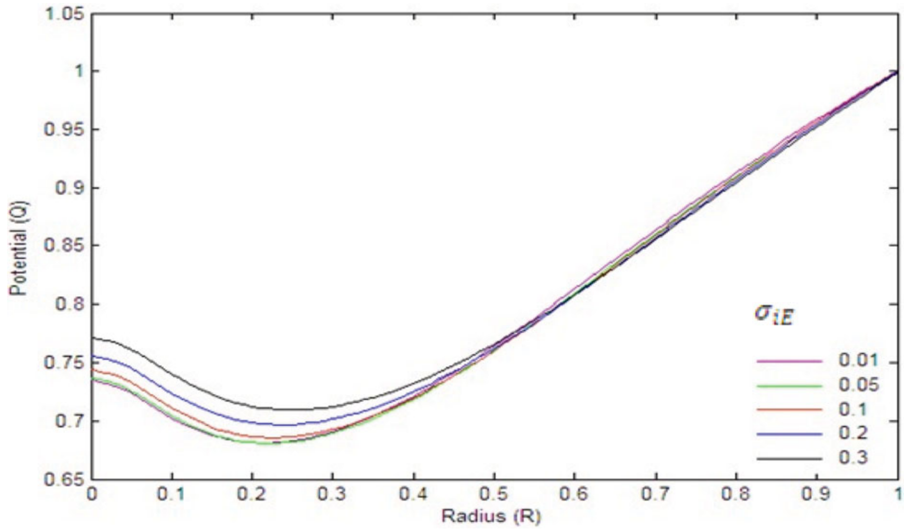

Figure 5. (Colour online) Dependence of radial potential well structure to σ_{iE}. ($\sigma_{eE} = 0.1$, $\sigma_{eQ} = 0.001$,$\sigma_{iQ} = 0.15$, $\beta = 0.2$, $P_i = 2$, and $\eta = 0.9$).

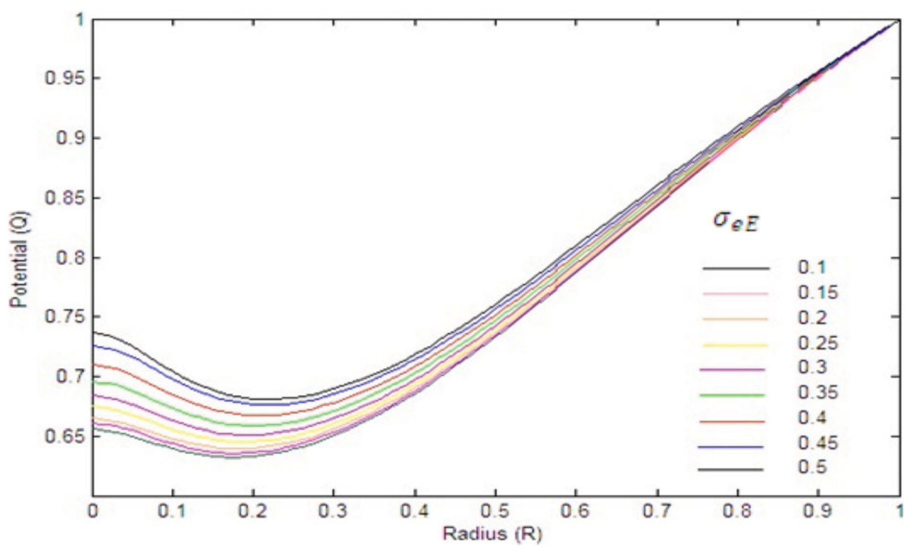

Figure 6. (Colour online) Dependence of radial potential well structure to σ_{eE}. ($\sigma_{eQ} = 0.001$, $\sigma_{iE} = 0.05$, $\sigma_{iQ} = 0.15$,$\beta = 0.2$,$P_i = 2$, and $\eta = 0.9$).

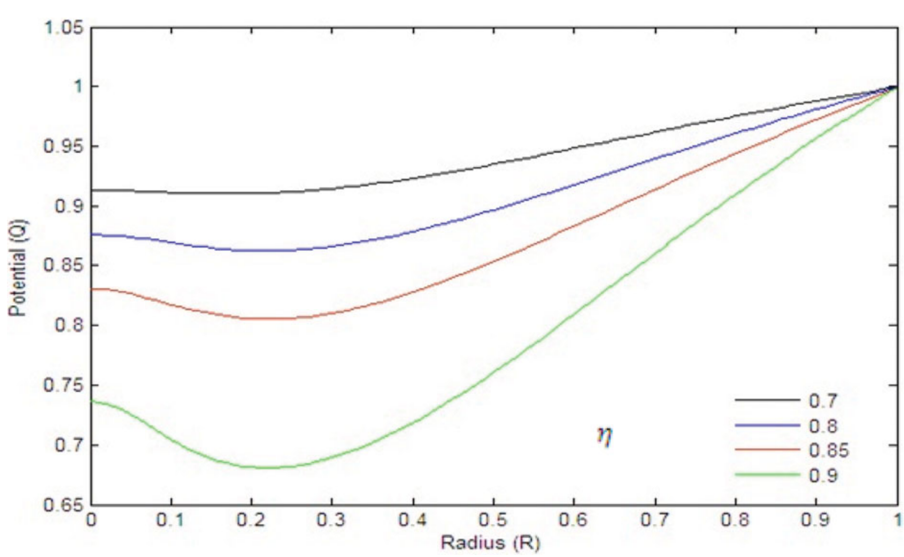

Figure 7. (Colour online) Dependence of radial potential well structure to η. ($\sigma_{eE} = 0.1$, $\sigma_{eQ} = 0.001$, $\sigma_{iE} = 0.05$, $\sigma_{iQ} = 0.15$, $\beta = 0.2$, and $P_i = 2$).

https://doi.org/10.1017/S002237781200092X Published online by Cambridge University Press

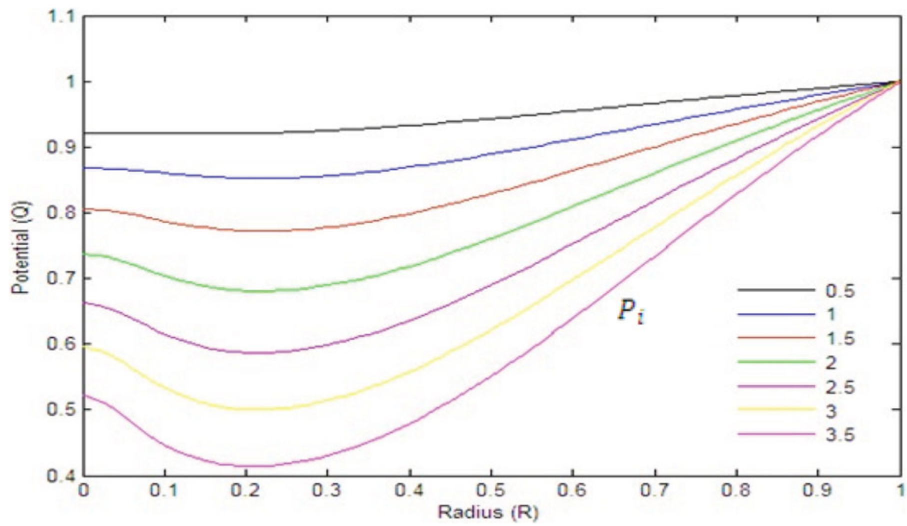

Figure 8. (Colour online) Dependence of radial potential well structure to P_i. ($\sigma_{eE} = 0.1$, $\sigma_{eQ} = 0.001$, $\sigma_{iE} = 0.05$, $\sigma_{iQ} = 0.15$, $\beta = 0.2$, and $\eta = 0.9$).

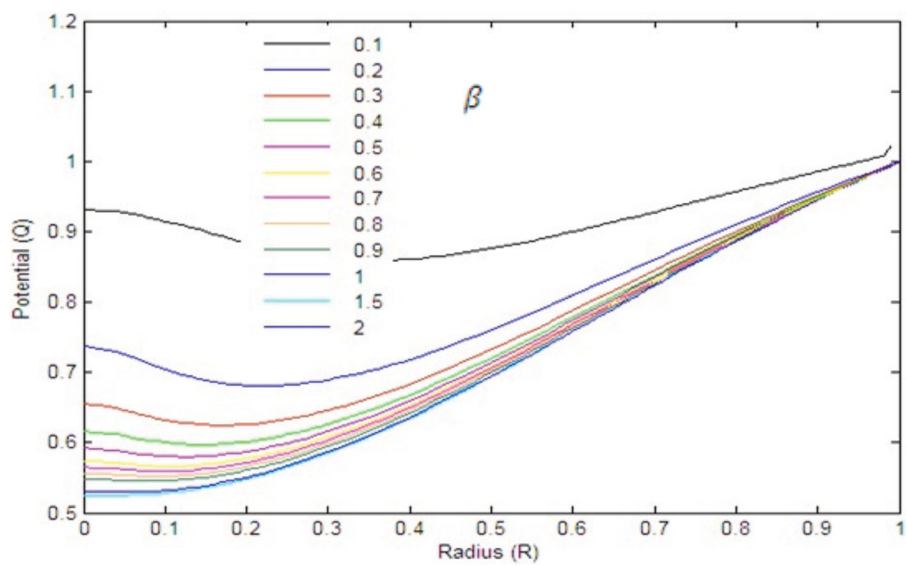

Figure 9. (Colour online) Dependence of radial potential well structure to β. ($\sigma_{eE} = 0.1$, $\sigma_{eQ} = 0.001$, $\sigma_{iE} = 0.05$, $\sigma_{iQ} = 0.15$, $P_i = 2$, and $\eta = 0.9$).

calculated. The constant control variables are $\sigma_{eE} = 0.1, \sigma_{eQ} = 0.001$, $\sigma_{iE} = 0.05$, $\sigma_{iQ} = 0.15$, $\beta = 0.2$, $P_i = 2$, and $\eta = 0.9$ in this work.

4. Results and discussion

Spreads in ion angular energy (σ_{iQ}) and electron angular energy (σ_{eQ}) had significant impact on the potential structure as seen in Figs. 3 and 4. The central peak of the double potential well failed to spot as a result of increasing electron angular energy (σ_{eQ}). So the strong dependence of double potential well on electron angular energy (σ_{eQ}) was well justified. Decreasing the ion angular energy (σ_{iQ}) increases the depth of the well.

Spreads in ion total energy (σ_{iE}) and electron total energy (σ_{eE}) had negligible influence on the potential well structure as displayed in Figs. 5 and 6. The dependence of potential well structure on grid transparency (η) is illustrated in Fig. 7. Decreasing this parameter causes a vanishing of the central peak of double potential well. Dependence of well structure on ion perveance is illustrated in Fig. 8. It is obvious from Fig. 9 that β is the other important parameter. Increasing this parameter puts down the existence of double potential well.

5. Conclusion

In this study, the analysis regarding potential structure of the IECF devices is presented. The theoretical analysis regarding potential well structure on the IECF devices has been carried out by solving Poisson equation for negatively biased grid as cathode placed at the center surrounded by anode in the presence of both ion and electron currents. Evaluations of potential well structure dependence on the electron and ion parameters to realize and predict the ions confinement are essential and are considered in this study. So we assumed $\sigma_{eE}, \sigma_{eQ}, \sigma_{iE}, \sigma_{iQ}$, η, P_i, and β as control parameters and evaluated the variation in radial potential well structure. According to our results, spreads in electron angular energy (σ_{eQ}) and ion angular energy (σ_{iQ}) had significant impact on the potential well structure and the strong dependence of double potential well structure on electron angular energy (σ_{eQ}) obtained. We showed that spreads in ion total energy (σ_{iE}) and electron total energy (σ_{eE}) had negligible influence on the potential well structure. The dependence of potential well structure on grid transparency (η), the injected ions current (P_i), and β are the other important parameters considered in this study.

References

Black, W. M. and Klevans, E. H. 1974 Theory of potential-well formation in an electrostatic confinement device. *J. Appl. Phys.* **45**, 2502.

Black, W. M. and Robinson, J. W. 1974 Measuring rotationally symmetric potential profiles with an electron-beam probe. *J. Appl. Phys.* **45**, 2497.

Cherrington, B. E. and Swanson, D. A. 1977 Theory of the multiple potential well structure created by bipolar injection in spherical geometry. *Phys. Fluids* **20**, 2139.

Cipiti, B. B. and Kulcinski, G. L. 2003 Embedded D-3He fusion reactions and medical isotope production in an inertial electrostatic confinement device. *Fusion Sci. Technol.* **44**, 534.

Dolan, T. J. 1975 Electrostatic-inertial plasma confinement. *PhD thesis.* University of Illinois, Urbana-Champaign.

Dolan, T. J., Verdeyen, J. T., Meeker, D. J. and Cherrington, B. E. 1972 electrostatic-inertial plasma confinement. *J. Appl. Phys.* **43**, 1590.

Elmore, W. C., Tuck, J. L. and Watson, K. M. 1959 On the inertial—electrostatic confinement of a plasma. *Phys. Fluids* **2**, 239–246.

Evstatiev, E. G., Nebel, R. A., Chacon, L., Park, J. and Lapenta, G. 2007 Space charge neutralization in inertial electrostatic confinement plasmas. *Phys. Plasmas* **14**, 042701.

Farnsworth, P. T. 1966 Electric discharge device for producing interactions between nuclei. US Patent 3 258 402.

Gu, Y. and Miley, G. H. 2000 Experimental study of potential structure in a spherical IEC fusion device. *IEEE Trans. Plasma. Sci.* **28**, 331–346.

Hirsch, R. L. 1967 Inertial electrostatic confinement of ionized fusion gases. *J. Appl. Phys.* **38**, 4522.

Hirsch, R. L. 1968 Experimental studies of a deep negative electrostatic potential well in spherical geometry. *Phys. Fluids* **11**, 2486.

Hockney, R. W. 1968 Formation and stability of virtual electrodes in a cylinder. *J. Appl. Phys.* **39**, 4166.

Hu, K. M. and Klevans, E. H. 1974 On the theory of electrostatic confinement of plasmas with ion injection. *Phys. Fluids* **17**, 227.

Kulcinski, G. L. 1996 Near term commercial opportunities from long range fusion research. *Fusion Technol.* **30**, 411.

Matsuo, T., Matsuura, H., Nakao, Y. and Kudo, K. 2004 Dependence of neutron/proton production rate on discharged current in spherical inertial electrostatic confinement plasma. *J. Plasma Fusion Res.* **6**, 731–734.

Matsuura, H., Funakoshi, K. and Nakao, Y. 2003 Correlation between ion/electron distribution functions and neutron production rate in spherical inertial electrostatic confinement plasmas. *Nucl. Fusion* **43**, 989.

Matsuura, H., Takaki, T., Funakoshi, K., Nakao, Y. and Kudo, K. 2000 Ion distribution function and radial profile of neutron production rate in spherical inertial electrostatic confinement plasmas. *Nucl. Fusion* **40**, 12.

Matsuura, H., Takaki, T., Nakao, Y. and Kudo, K. 2001 Radial profile of neutron production rate in spherical inertial electrostatic confinement plasmas. *Fusion Technol.* **39**, 1167.

Meyer, R. M., Loyalka, S. K. and Prelas, M. A. 2005 Potential well structure in spherical inertial electrostatic confinement device. *IEEE Trans. Plasma Sci.* **33**, 1377.

Momota, H. and Miley, G. H. 2001 Virtual cathode in a stationary spherical inertial electrostatic confinement. *Fusion Sci. Technol.* **40**, 56.

Nadler, J. H. 1992 Space-charge dynamics and neutron generation in an inertial- electrostatic confinement device. *PhD thesis.* University of Illinois, Urbana-Champaign.

Nebel, R. A., Stange, S., Park, J., Taccetti, J. M., Murali, S. K. and Garcia, C. E. 2005 Theoretical and experimental studies of kinetic equilibrium and stability of the virtual cathode in an electron injected inertial electrostatic confinement device. *Phys. Plasmas* **12**, 012701.

Nevins, W. M. 1995 Can inertial electrostatic confinement work beyond the ion-ion collisional time scale? *Phys. Plasmas* **2**, 3804.

Ohnishi, M., Sato, K. H., Yamamoto, Y. and Yoshikawa, K. 1997 Correlation between potential well structure and neutron production in inertial electrostatic confinement fusion. *Nucl. Fusion* **37**, 611.

Ohnishi, M., Yamamoto, Y., Hasegawa, M., Yoshikawa, K. and Miley, G. H. 1998 Study on an inertial electrostatic confinement fusion as a portable neutron source. *Fusion Eng. Des.* **42**, 207–211.

Swanson, D. A. 1975 Theoretical study of a spherical inertial electrostatic plasma confinement device. *PhD thesis.* University of Illinois, Urbana-Champaign.

Swanson, D. A., Cherrington, B. E. and Verdeyen, J. T. 1973a Potential well structure in an inertial electrostatic plasma confinement device. *Phys. Fluids* **16**, 1939.

Swanson, D. A., Cherrington, B. E. and Verdeyen, J. T. 1973b Multiple potential-well structure created by electron injection in spherical geometry. *Appl. Phys. Lett.* **23**, 125.

Taniuchi, Y., Matsumura, Y., Taira, K., Utsumi, M., Chiba, M., Shirakawa, T. and Fujii, M. 2010 Effect of grid cathode structure on a low-input-power inertial electrostatic confinement fusion device. *J. Nucl. Sci. Technol.* **47**, 626.

Thorson, T. A., Durst, R. D., Fonck, R. J. and Wainwright, L. P. 1997 Convergence electrostatic potential, and density measurement in a spherical convergent ion focus. *Phys. Plasmas* **4**, 4.

Tzonev, I. V., DeMora, J. M. and Miley, G. H. 1996 Effect of large ion angular momentum spread and high current on inertial electrostatic confinement potential structures. Paper 16th IEEE/NPSS Symp, Urbana, IL, 30 September–5 October 1995. *Fusion Engineering* **2**, 1476–1481.

Weidner, J. W. 2003 The production of 13N from inertial electrostatic confinement fusion. *MS thesis*, University of Wisconsin-Madison.

Wong, S. K. and Krall, N. A. 1992 Potential well formation by injection of electrons with various energy distributions into a sphere or a slab. *Phys. Fluids* B **4**, 4140.

Yamamoto, Y., Hasegawa, M., Ohnishi, M., Yoshikawa, K. and Inoue, N. 1997 Preliminary studies of potential well measurement in inertial-electrostatic confinement fusion experiments. Paper 17th IEEE/NPSS Symp. *Fusion Engineering* **2**, 745–748.

Yoshinaga, S., Matsuura, H., Nakao, Y. and Kudo, K. 2006 Energy distribution of fast neutral atoms and neutron production rate in inertial electrostatic confinement device. *J. Plasma Fusion Res.* **7**, 127–130.

https://doi.org/10.1017/S002237781200092X Published online by Cambridge University Press